

10 PW 激光装置终端聚焦光场参数的测量与优化

尤金昌^{1,2}, 於亮红^{1*}, 孙奕杰¹, 樊超¹, 张晓波¹, 姚波¹, 梁晓燕^{1**}¹中国科学院上海光学精密机械研究所强场激光物理国家重点实验室, 上海 201800;²上海科技大学物质科学与技术学院, 上海 201210

摘要 聚焦光场强度是超强超短激光与物质相互作用实验中最为核心的技术指标之一。本文提出了 10 PW 激光系统在真空条件下聚焦光场的参数测量方案, 解决了终端物理靶场在真空环境中难以实现激光参数准确测量的难题。该方案通过平场消色差物镜和大口径光学器件优化设计, 降低了取样测量系统引入的色差和单色像差。利用理想光源对取样测量系统进行标定, 结果显示, 该系统引入的波前畸变峰谷值(PV 值)为 0.106 μm , 均方根值(RMS 值)为 0.016 μm , 接近测量仪器的最小极限值, 对主激光测量误差的影响可以忽略。同时, 取样测量系统实现了终端变形镜与波前探测器的严格物像共轭关系, 保证了自适应光学系统波前校正效果最优。通过对比空气条件和真空条件下的波前和焦斑测量结果, 验证了取样测量系统的有效性。在真空条件下, 利用该取样测量系统对激光脉冲进行波前、焦斑测量和优化, 获得了接近衍射极限的聚焦焦斑。2.7 PW 激光脉冲经焦距为 2000 mm 的离轴抛物面镜聚焦后, 聚焦光强可达到 $4 \times 10^{21} \text{ W/cm}^2$, 能为物理实验提供极端的物理条件。

关键词 激光光学; 超快激光; 10 PW 激光系统; 焦场; 波前校正

中图分类号 TN247

文献标志码 A

DOI: 10.3788/CJL221042

1 引言

自 20 世纪 80 年代末啁啾脉冲放大技术(CPA)^[1]被提出后, 超强超短激光技术得到了迅速发展, 峰值功率从太瓦(TW)量级发展到拍瓦(PW)量级, 目前已发展到 10 PW^[2-4]。拍瓦级超强超短激光脉冲经过聚焦后会形成数微米直径的聚焦焦斑, 焦斑区域内的激光强度能够达到 $10^{20} \sim 10^{23} \text{ W/cm}^2$ ^[5-7], 可提供超强的电场、磁场以及巨大的光压等极端实验条件, 为高能粒子加速、高密度物理、实验室天体物理等前沿基础研究^[8-10]提供了前所未有的研究手段和研究平台。

上海超强超短激光实验装置^[11](SULF, 以下称“羲和激光装置”)于 2017 年实现了单次 10.3 PW 激光脉冲放大输出, 之后于 2019 年采用重复频率为 1 shot/min 的泵浦源进行泵浦, 再经钛宝石主放大器放大实现了约 400 J 的宽带激光脉冲放大输出, 宽带脉冲经四光栅压缩器压缩后获得了脉冲宽度为 21 fs、重复频率为 1 shot/min 的 10 PW 级超强超短激光脉冲输出。

压缩后的飞秒激光脉冲具有较高的光强, 超过了激光在空气中的电离阈值, 在空气中传输时会导

致激光光束质量严重劣化。因此, 压缩后的飞秒激光的传输及激光物理实验一般都在真空管道和真空腔体(真空度达到了 $10^{-4} \sim 10^{-5} \text{ Pa}$)内进行。调研结果显示, 目前大多数满足焦点探测的高动态 CCD 和波前探测器主要在大气环境下使用, 而在真空中使用的探测设备较少, 且价格昂贵。对聚焦光场的特性(比如激光的波前畸变和焦斑分布)进行准确测量, 是利用自适应光学优化激光波前畸变、提升激光聚焦性能的前提。因此, 为了给物理实验提供更加准确的激光参数, 需要实现真空条件下激光脉冲焦斑和波前等参数的测量, 以准确标定激光的聚焦光强。

目前, 相关文献对超强超短激光装置波前校正和聚焦优化介绍的比较多, 但是从物理实验应用的角度出发, 专门针对真空条件下激光靶场波前和焦场取样探测的文献较少, 而且缺乏对拍瓦级激光终端聚焦光场测量系统的性能分析。针对 10 PW 激光装置终端物理靶场, 笔者设计了一种在真空条件下对聚焦激光脉冲进行取样测量的系统。该取样测量光学系统可以保证终端变形镜与波前探测器处于成像关系, 不仅能够真空条件下对激光脉冲的波前畸变进行测量与校正, 还能将聚焦的焦斑在空间上放大 10 倍后进行精确

收稿日期: 2022-07-13; 修回日期: 2022-09-02; 录用日期: 2022-11-14; 网络首发日期: 2022-11-24

基金项目: 国家自然科学基金(61775223, 11804349)、上海市科学技术创新计划(19142202500)、中国科学院先导战略研究计划(XDB1603)、中国科学院青年创新促进会资助项目(2019247)

通信作者: *lhyu@siom.ac.cn; **liangxy@siom.ac.cn

测量。该取样系统自身引入的波前畸变的峰谷值(PV值)不大于 $0.1\ \mu\text{m}$,均方根值(RMS值)不大于 $0.02\ \mu\text{m}$,能够较为真实地反映物理实验中10 PW主激光的真实状态,为激光与物质相互作用实验的开展提供了准确的测量手段。

2 取样测量系统设计

羲和激光装置10 PW激光系统是基于钛宝石晶体啁啾脉冲放大技术实现的。激光脉冲经钛宝石主放大器放大后,能量约为400 J。为避免压缩光栅发生损坏,激光光斑由180 mm扩束至500 mm^[11-12],之后被四光栅压缩器压缩至30 fs以下,形成10 PW激光脉冲。压缩后的10 PW激光脉冲先经过通光口径为520 mm的可变形镜(DM)^[13],再经过若干反射镜传输至离轴抛物面镜(OAP)进行聚焦^[14-15],形成与靶材相互作用的聚焦焦斑。在激光与物质相互作用的实验中,激光聚焦的焦斑区域是激光与物质相互作用的靶场,开展物理实验研究时该区域须处于真空环境下。因此,如何在真空条件下对靶场焦斑进行取样测量并校正波前,是进行激光与物质相互作用实验的重要前提条件。

本系统可以在空气和真空条件下对焦斑的波前和强度分布进行取样测量,并且可以将测量的取样波前反馈至可变形镜上,对激光光束的波前畸变进行校正,提升激光装置的聚焦性能。该系统光路如图1所示,10 PW激光经过焦距为2000 mm(F 数为4)的离轴抛物面镜聚焦,聚焦后的激光脉冲在焦点后经过一块高精度物镜^[16](10 \times),输出直径为5 mm的准直光束。该物镜与后续的两块反射镜固定在一个真空兼容的一维线性电动平移台上。该平移台可以实现在真空条件下的推进和推出,推进时可以对激光参数取样测量,推出后激光可用于物理实验。该平移台的最大行程为450 mm,重复定位精度不大于 $2.5\ \mu\text{m}$,可以确保取样光路在激光测量与物理实验之间切换,并且能够保证高精度切换。

10 PW激光装置物理靶室的空间尺寸大,激光聚焦焦斑位置距离靶室窗片2~3 m。为保障真空传输后的光束质量以及变形镜与波前探测器的成像关系,须对取样后的激光脉冲进行像传递传输。离轴抛物面镜和物镜组成一级像传递系统,它可将变形镜表面的像传递至物镜,之后,变形镜表面的像经消色差透镜L1和L2组成的1:1二级像传递系统进一步传递至真空靶室外的波前探测器接收面上。激光光束经过两级像传递后,再经过窗片传输至真空靶室外的空气中。激光光束经过两级像传递后,再经过窗片传输至真空靶室外的空气中。激光再经过高光束质量分光镜(透反比为7:3)进行分光,透射部分的激光传输至波前探测器,反射部分的激光经消色差透镜(目镜,焦距为200 mm)会聚后被CCD探测。波前探测器(WFS,中国科学院光电技术

研究所研制)和CCD(SP928,OPHIR公司生产)均位于空气环境中。

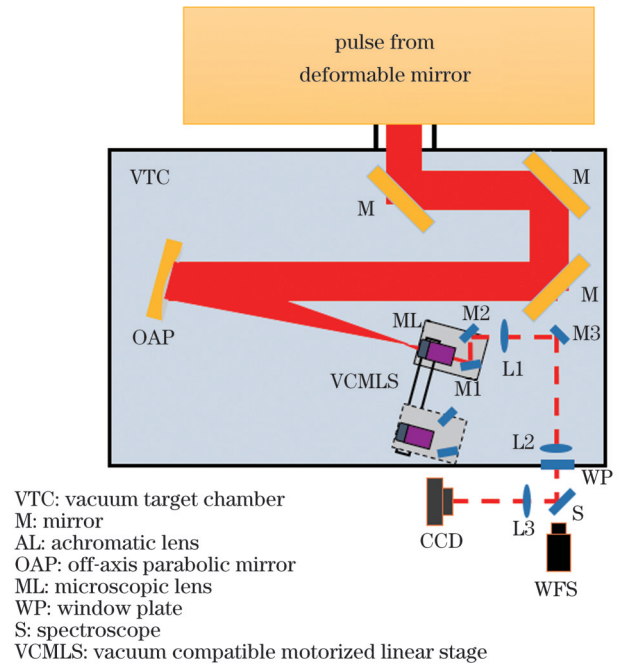


图1 真空焦场取样测量系统示意图

Fig.1 Schematic of vacuum focal field sampling measurement system

2.1 色差和单色像差设计

10 PW激光脉冲的光谱范围为 $800\ \text{nm} \pm 50\ \text{nm}$,在设计过程必须要考虑光学器件的消色差设计^[14]。物镜采用的是日本Mitutoyo公司生产的近红外平场消色差物镜,该系列物镜可以在整个视场内提供平面的、无单色像差的成像质量^[16]。为进一步降低取样系统引入的色差和单色像差,设计时在5 mm光束口径光路中采用了50 mm口径的光学器件,利用光学器件的局部高面型精度来进一步降低取样光路对波前的影响。对除了物镜外的光路进行光线追踪,得到了图2所示的光程差(OPD)图。可以看到,不同波长导致的色差不大于 0.002λ ,最大单色像差不大于 0.0065λ ,色差和单色像差可以忽略。

2.2 像传递设计

在自适应光学系统^[17]中,变形镜的镜面和波前探测器的接收面应保持成像共轭关系,这样才能保障波前校正效果达到最优。在10 PW激光系统中,变形镜安装在物理靶室前的激光品质提升的真空腔体内,距离离轴抛物面镜15.8 m。离轴抛物面镜和物镜组成一级像传递系统,L1和L2组成二级像传递系统,变形镜表面与波前探测器接收面保持严格的成像关系。为了检验变形镜镜面与波前探测器接收面是否为像共轭关系,在变形镜表面插入薄纸片,通过CCD上像的清晰度来判断变形镜镜面与波前探测器是否严格处于像共轭位置。如图3所示,薄纸边缘成像比较清晰,成

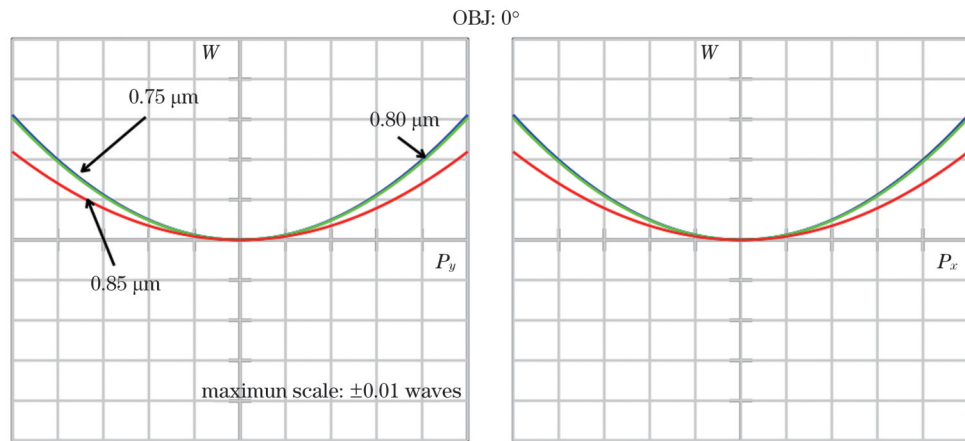


图2 基于Zemax的取样光路波像差的优化结果(不包含物镜),其中蓝色曲线表示750 nm波长,绿色曲线表示800 nm波长,红色曲线表示850 nm波长

Fig. 2 Wave aberration optimization results of sampling optical path based on Zemax (without objective lens). Blue, green, and red curves denote 750 nm, 800 nm, and 850 nm, respectively

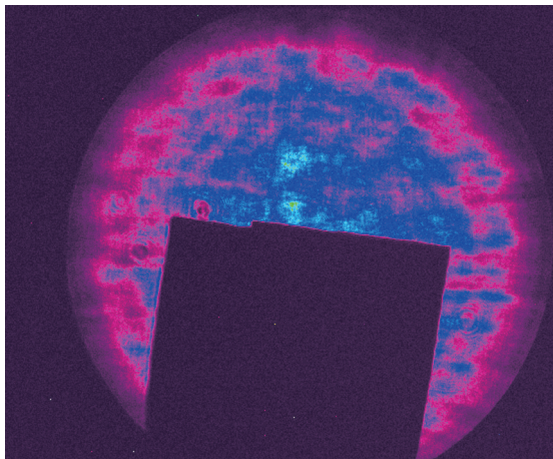


图3 变形镜和波前探测器成像共轭关系测试

Fig. 3 Test of image conjugate relationship between deformable mirror (DM) and wavefront sensor (WFS)

像质量较好,由此可以定性地判断波前探测器处于最佳的成像位置。

2.3 取样测量系统自身波前畸变的标定

基于焦斑处的取样测量系统可以对整个激光系统的光学器件(包括变形镜后的反射镜和离轴抛物面镜)引入的波前畸变量进行测量和校正,从而获得最理想的聚焦焦斑。但是,如果取样系统自身引入的波前畸变量过大,将会对主激光的波前校正带来不利影响。为了保证取样测量光路的可靠性,须对取样光路进行严格设计:1) 光学器件的设计和加工必须严格控制,以保证器件的质量,要求单块透镜和反射镜的加工面型质量为PV值不大于 $\frac{1}{10}\lambda$ 且RMS不大于

$\frac{1}{60}\lambda$ ($\lambda=632.8\text{ nm}$); 2) 为避免装校过程中产生波前误差,必须严格按照优化设计的光路进行光学器件的装调。光路完成后,采用光纤输出的半导体激光器作

为理想光源对取样光路系统进行标定,该光源的PV值约 $0.102\text{ }\mu\text{m}$,RMS值约 $0.014\text{ }\mu\text{m}$,接近标定仪器四波剪切干涉仪(SID4)^[18]的测量极限。光纤输出头固定在五维调整架上,通过精密调节以及对波前探测器、CCD上的远近场定标,可以实现光纤输出光路与主激光在取样光路中高度重合。测量的参考激光的波前畸变和远场分布如图4所示。参考光的PV值为 $0.106\text{ }\mu\text{m}$,RMS值为 $0.016\text{ }\mu\text{m}$,接近波前探测器的测量极限值。采用Ophir公司生产的型号为SP928的科研级CCD(模数转换器的分辨率为12 bit,单像素点尺寸为 $3.69\text{ }\mu\text{m}$)对经过取样光路后的参考光远场进行测量,远场聚焦尺寸($1/e^2$)约为 $60\text{ }\mu\text{m}$ 。根据设计光纤输出的点光源尺寸 $5.5\text{ }\mu\text{m}\pm 0.5\text{ }\mu\text{m}$,得到取样测量系统的放大倍率约为10倍,远场聚焦接近衍射极限。

3 实验结果分析

为了避免器件的损伤和非线性效应,该取样系统必须工作在宽带飞秒激光为低能量的条件下,因此需要对激光脉冲进行能量衰减。由前期研究可知,基于CPA技术的脉冲放大对波前畸变的劣化程度较小^[19],静态测量的波前畸变能够较好地反映动态波前畸变的变化。所以,通过降低前端泵浦能量以及使主放大器泵浦不工作来降低系统的输出能量,并在输出端用一块高质量白板(PV不大于 0.1λ)对激光能量进行进一步衰减。衰减后的主激光经过取样光路的分光镜后,透射部分进入波前探测器测量波前并用于波前校正,反射部分被高动态范围CCD接收用于测量焦斑强度分布。图5为校正前通过取样测量系统在空气条件和真空条件下测量的激光波前。表1为校正前基于图5测量结果得到的PV值、RMS值和前三阶Zernike多项式系数。对比取样光路在空气条件和真空条件下校正

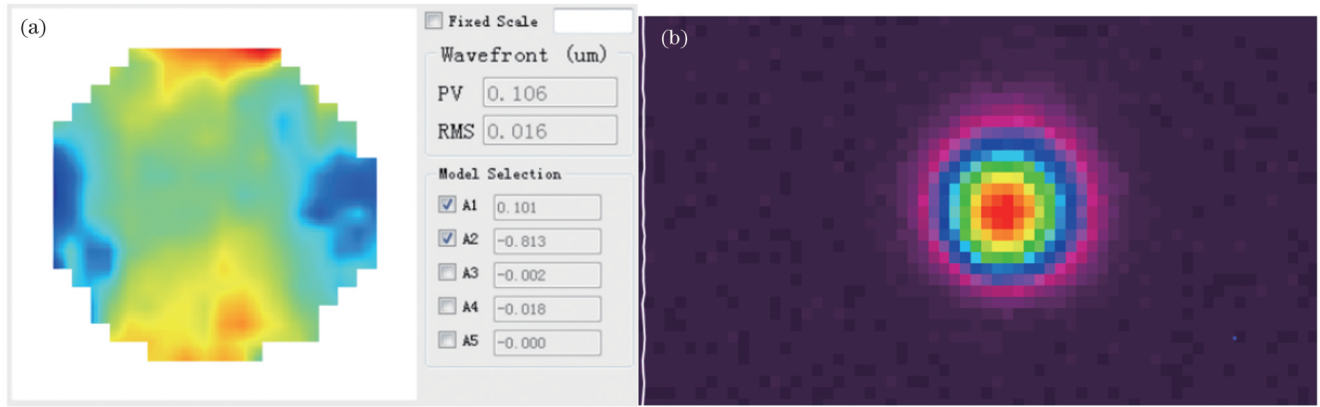


图 4 理想参考光(780 nm)通过取样系统后的参数测量图。(a)波前畸变;(b)远场分布

Fig.4 Parameters diagrams of ideal reference light (780 nm) after passing through sampling system. (a) Wavefront distortion; (b) far-field distribution

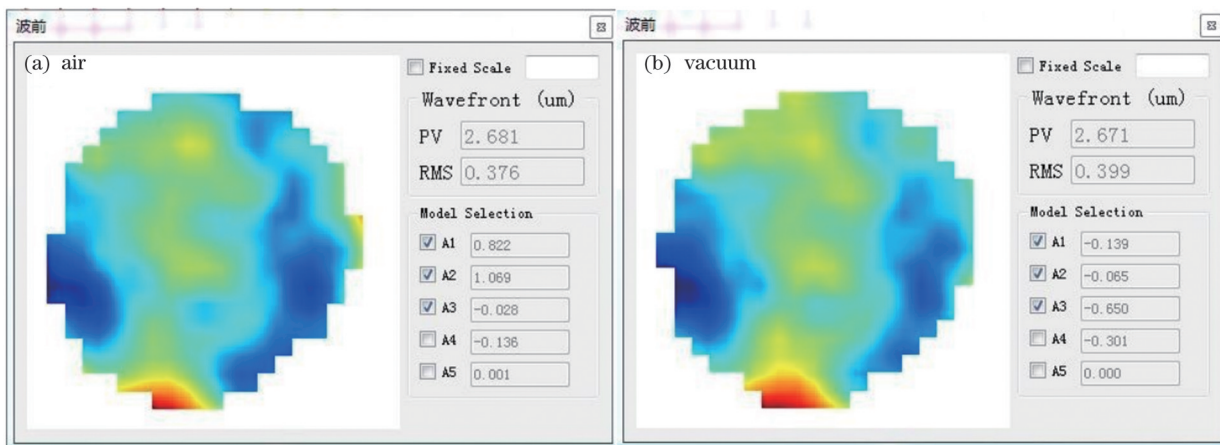


图 5 可变形镜校正前,取样测量系统在空气和真空条件下测量的波前

Fig.5 Wavefront measured by sampling measurement system under air and vacuum conditions before deformable mirror correction

前的波前畸变分布及相应的 PV 值、RMS 值和前三阶 Zernike 多项式系数(A3、A4、A5 分别代表 Power、Astig X、Astig Y)可以看到,除 A3 系数外,空气和真空条件下的数据都非常接近。Power 项的变化比较大,这主要是由压缩器腔体上的窗片在真空条件下发生的微小形变引起的,它会引入焦斑固定的纵向移动。这表明真空条件下和空气条件下的焦点位置虽然有微小差别,但不影响激光脉冲聚焦光束的质量以及物理实验的开展。测量结果表明该取样测量系统能够较好地完成真空条件下对 10 PW 激光光束的波前测量工作。

表 1 波前校正前,空气和真空条件下测量的波前 PV、RMS 和前三阶 Zernike 多项式系数

Table 1 PV, RMS and the first third-order Zernike polynomial coefficients of measured wavefront under air and vacuum conditions before wavefront correction

Condition	PV / μm	RMS / μm	Power	Astig X	Astig Y
Air	2.681	0.376	-0.028	-0.136	0.001
Vacuum	2.671	0.399	-0.650	-0.301	0

利用该取样光路系统对 10 PW 激光脉冲进行波前校正,基于终端的 520 mm 口径可变形镜可将激光波前畸变由校正前的数值降低至 PV 为 0.5 μm 和 RMS 值为 0.07 μm 。采用焦距为 2000 mm 的离轴抛物面镜聚焦之后,在空气和真空条件下获得了如图 6 所示的聚焦焦斑分布。由图 6 可见,在相同的变形镜校正电压下,空气和真空条件下均能获得接近衍射极限的激光聚焦焦斑。

该取样光路为 10 PW 激光系统终端的高能质子加速实验提供了比较准确的波前和焦斑测量参数。采用该取样光路对主激光焦场的波前和焦斑进行测量,并将测量结果反馈至自适应光学控制系统,通过控制变形镜的面型改变来优化最终的焦场,在激光系统输出为 2.7~3 PW 时,激光的最高聚焦光强达到了 $4 \times 10^{21} \text{ W/cm}^2$,物理实验获得了 62 MeV 的高能质子输出^[20]。最终的物理实验结果验证了 10 PW 终端聚焦光场参数测量与优化的有效性。

4 结 论

设计了可在真空条件下测量激光波前和焦斑等参

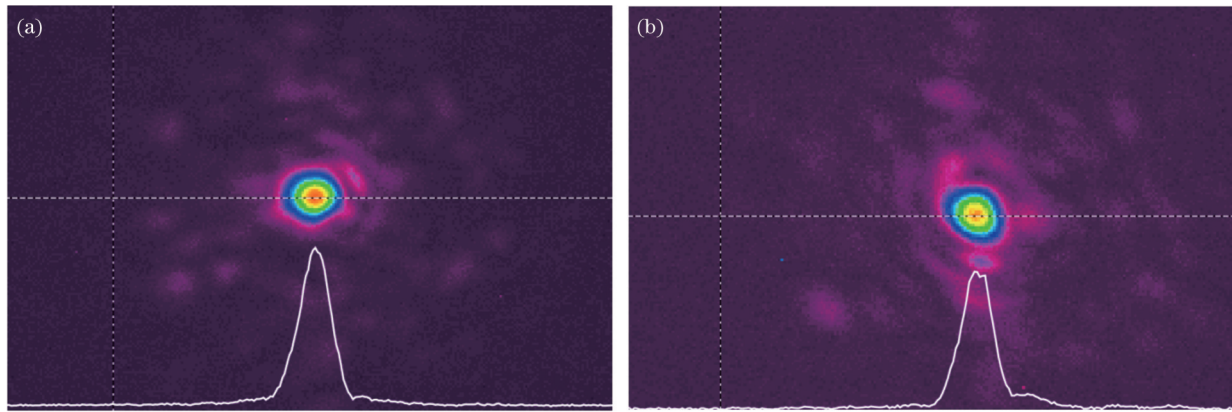


图 6 用可变形镜进行波前校正后测量的焦斑。(a)空气条件下;(b)真空条件下

Fig.6 Focal spot measured after wavefront correction by deformable mirror. (a) Under air condition; (b) under vacuum condition

数的取样测量系统,并利用该系统在真空条件下对激光波前及焦斑进行了优化与测量。理论设计与实验测量结果表明,该取样测量系统引入的色差及波前畸变基本可以忽略,能够比较准确地反映主激光的波前畸变及真空下的焦场特性。10 PW 主激光在空气和真空条件下的波前测量结果表明,该系统在真空下测量的波前畸变与在空气中测量的波前畸变基本保持一致。利用该系统在真空条件下对 10 PW 激光脉冲聚焦焦斑进行测量和校正,得到了接近衍射极限的聚焦焦斑。该系统可为物理实验的开展提供比较准确的焦场信息测量结果。

参 考 文 献

- [1] Strickland D, Mourou G. Compression of amplified chirped optical pulses[J]. *Optics Communications*, 1985, 55(6): 447-449.
- [2] Chu Y X, Liang X Y, Yu L H, et al. High-contrast 2.0 Petawatt Ti:sapphire laser system[J]. *Optics Express*, 2013, 21(24): 29231-29239.
- [3] Sung J H, Lee H W, Yoo J Y, et al. 4.2 PW, 20 fs Ti:sapphire laser at 0.1 Hz[J]. *Optics Letters*, 2017, 42(11): 2058-2061.
- [4] Gan Z B, Yu L H, Li S, et al. 200 J high efficiency Ti:sapphire chirped pulse amplifier pumped by temporal dual-pulse[J]. *Optics Express*, 2017, 25(5): 5169-5178.
- [5] Bahk S W, Rousseau P, Planchon T A, et al. Characterization of focal field formed by a large numerical aperture paraboloidal mirror and generation of ultra-high intensity (10^{22} W/cm²) [J]. *Applied Physics B*, 2005, 81(5): 727.
- [6] Guo Z, Yu L H, Wang J Y, et al. Improvement of the focusing ability by double deformable mirrors for 10-PW-level Ti:sapphire chirped pulse amplification laser system[J]. *Optics Express*, 2018, 26(20): 26776-26786.
- [7] Yoon J W, Kim Y G, Choi I W, et al. Realization of laser intensity over 10^{23} W/cm²[J]. *Optica*, 2021, 8(5): 630-635.
- [8] Wang W T, Li W T, Liu J S, et al. High-brightness high-energy electron beams from a laser wakefield accelerator via energy chirp control[J]. *Physical Review Letters*, 2016, 117(12): 124801.
- [9] Kim I J, Pae K H, Choi I W, et al. Radiation pressure acceleration of protons to 93 MeV with circularly polarized petawatt laser pulses [J]. *Physics of Plasmas*, 2016, 23(7): 070701.
- [10] Jiao J, Zhang B, Yu J, et al. Generating high-yield positrons and relativistic collisionless shocks by 10 PW laser[J]. *Laser and Particle Beams*, 2017, 35(2): 234-240.
- [11] Li W Q, Gan Z B, Yu L H, et al. 339 J high-energy Ti:sapphire chirped-pulse amplifier for 10 PW laser facility[J]. *Optics Letters*, 2018, 43(22): 5681-5684.
- [12] Gan Z B, Yu L H, Wang C, et al. The Shanghai Superintense Ultrafast Laser Facility (SULF) project[M]// *Progress in Ultrafast Intense Laser Science XVI*. Cham: Springer, 2021: 199-217.
- [13] 王建设, 郭震, 於亮红, 等. 10 PW 级激光系统波前演变及分析 [J]. *中国激光*, 2019, 46(8): 0801006.
- [14] Wang J Y, Guo Z, Yu L H, et al. Wavefront evolution and analysis of 10-petawatt laser system[J]. *Chinese Journal of Lasers*, 2019, 46(8): 0801006.
- [15] Bor Z. Distortion of femtosecond laser pulses in lenses and lens systems[J]. *Journal of Modern Optics*, 1988, 35(12): 1907-1918.
- [16] Zeng X H, Chen X Y. Characterization of tightly focused vector fields formed by off-axis parabolic mirror[J]. *Optics Express*, 2019, 27(2): 1179-1198.
- [17] Moser J. Microscope objectives[J]. *Photoniques*, 2021(107): 59-64.
- [18] Jiang W H, Li H G. Hartmann-Shack wavefront sensing and wavefront control algorithm[J]. *Proceedings of SPIE*, 1990, 1271: 82-93.
- [19] Chanteloup J C F, Cohen M. Compact high resolution four wave lateral shearing interferometer[J]. *Proceedings of SPIE*, 2004, 5252: 282-292.
- [20] Guo Z, Yu L H, Li W Q, et al. Wavefront evolution of the signal beam in Ti:sapphire chirped pulse amplifier[J]. *Chinese Physics B*, 2019, 28(1): 014203.
- [21] Li A X, Qin C Y, Zhang H, et al. Acceleration of 60 MeV proton beams in the commissioning experiment of SULF-10 PW laser[J]. *High Power Laser Science and Engineering*, 2022, 10: 1-20.

Measurement and Optimization of Terminal Focusing Optical Field Parameters of a 10 PW Laser Device

You Jinchang^{1,2}, Yu Lianghong^{1*}, Sun Yijie¹, Fan Chao¹, Zhang Xiaobo¹, Yao Bo¹,
Liang Xiaoyan^{1**}

¹State Key Laboratory of High Field Laser Physics, Shanghai Institute of Optics and Fine Mechanics, Chinese Academy of Sciences, Shanghai 201800, China;

²School of Physical Science and Technology, ShanghaiTech University, Shanghai 201200, China

Abstract

Objective Focused light field parameters are the core indices for the interaction experiments between ultra-intense ultrashort lasers and matter, and they are also a prerequisite for correcting wavefront distortion and optimizing the focusing performance via adaptive optics. Presently, several studies introduce the parameters of ultra-intense ultrashort laser devices. However, from an application perspective in physical experiments, there are very few reports on the sampling and measurement of the laser wavefront and focal point under vacuum conditions. In this study, a scheme for sampling and measuring the focused light field in a target chamber under vacuum conditions and exposure to a 10 PW laser device is presented. Through the fixing of some elements on the translation table, switching between parameter measurements and physical experiments is realized. Moreover, the measurement system has a high measurement accuracy and provides more accurate laser parameters for physical experiments.

Methods The optical path of the sampling measurement system was designed and built. First, according to the wide spectrum characteristics of the laser pulse, an achromatic objective lens and a large-aperture achromatic lens were used to reduce the chromatic aberration that may be introduced by the system. Second, to ensure the optimality of adaptive optical wavefront correction, an image transfer system was designed to ensure the occurrence of an object-image conjugate relationship between the deformable mirror and wavefront detector. Subsequently, an ideal light source was used to calibrate the wavefront distortion introduced by the sampling measurement system. Finally, the focused light field in the target chamber was measured and optimized under air and vacuum conditions.

Results and Discussions After completing the optical path, a semiconductor laser output from the optical fiber is used as the ideal light source to calibrate the sampling measurement system. The peak-valley (PV) value of the light source is $0.102\ \mu\text{m}$, and the RMS value is $0.014\ \mu\text{m}$, which is close to the measurement limit of the four-wave shear interferometer device. The size of point light source is $5.5\ \mu\text{m} \pm 0.5\ \mu\text{m}$, and the measured far-field focusing size is approximately $60\ \mu\text{m}$ after 10 times magnification, which is close to the diffraction limit (Fig. 4). Subsequently, wavefront measurements of the main laser are conducted under air and vacuum conditions before undergoing correction, and the difference in the results shows the necessity of vacuum sampling measurement (Fig. 5). The wavefront correction of the 10 PW laser pulse is performed using a sampling optical path system. The deformable mirror (520 mm) reduces the peak-valley (PV) value to $0.5\ \mu\text{m}$ and the root-mean-square (RMS) value to $0.07\ \mu\text{m}$. Under the same correction voltage, the laser focus point closest to the diffraction limit can be obtained under both air and vacuum conditions (Fig. 6).

Conclusions In this study, a sampling measurement system is designed and built to measure the laser-focused light field in vacuum. The design and calibration results show that the system introduces minimal chromatic aberration and wavefront distortion, and it can accurately measure the wavefront distortion and intensity distribution of the laser focal field. The results of the wavefront measurement in air and in vacuum using the 10 PW main laser show that the wavefront distortion measured by this system in vacuum is essentially consistent with that in air, and the slight difference in the Zernike coefficient indicates the necessity of the system. Using this system, the wavefront of the 10 PW laser pulse focus point is measured and corrected under air and vacuum conditions, and the focus point closest to the diffraction limit is obtained, which proves the effectiveness of the sampling measurement system. In summary, the proposed system can accurately measure the wavefront distortion and intensity distribution of a 10 PW laser focal field under physical experimental conditions and perform wavefront correction through an adaptive optics system to improve the laser focusing performance. It also provides accurate laser parameters and extreme physical conditions for investigating the interactions between strong light and matter.

Key words laser optics; ultrafast lasers; 10 PW laser system; foael field; wavefront correction